

22. Watts, A. B. An analysis of isostasy in the world's oceans: 1. Hawaiian-Emperor seamount chain. *J. Geophys. Res.* **83**, 5989–6004 (1978).
23. Wessel, P. A reexamination of the flexural deformation beneath the Hawaiian swell. *J. Geophys. Res.* **98**, 12177–12190 (1993).
24. Jackson, E. D. & Shaw, H. R. Stress fields in central portions of the Pacific plate: Delineated in time by linear volcanic chains. *J. Geophys. Res.* **80**, 1861–1874 (1975).
25. Hauri, E. H. Major-element variability in the Hawaiian mantle plume. *Nature* **382**, 415–419 (1996).
26. Wessel, P. & Kroenke, L. A geometric technique for relocating hotspots and refining absolute plate motions. *Nature* **387**, 365–369 (1997).
27. Canuto, C., Hussaini, M. Y., Quarteroni, A. & Zang, T. A. *Spectral Methods in Fluid Dynamics* (Springer, New York, 1988).
28. Jaeger, J. C. & Cook, N. G. W. *Fundamentals of Rock Mechanics* 3rd edn 190–191 (Chapman & Hall, London, 1979).
29. Swanson, D. A. Magma supply rate at Kilauea volcano, 1952–1971. *Science* **175**, 169–170 (1972).

**Acknowledgements.** We thank N. Ribe, A. Rubin and Y. Ricard for helpful comments. This work was supported by the NSF.

Correspondence and requests for materials should be addressed to D.B. (e-mail: dberco@soest.hawaii.edu).

## A primitive fossil fish sheds light on the origin of bony fishes

Min Zhu\*, Xiaobo Yu† & Philippe Janvier‡

\* Institute of Vertebrate Paleontology and Paleoanthropology, Chinese Academy of Sciences, PO Box 643, Beijing 100044, China

† Department of Biological Sciences, Kean University, Union, New Jersey 07083, USA

‡ URA12, Laboratoire de Paléontologie, Muséum National d'Histoire Naturelle, 8 rue Buffon, 75005 Paris, France

Living gnathostomes (jawed vertebrates) include chondrichthyans (sharks, rays and chimaeras) and osteichthyans or bony fishes. Living osteichthyans are divided into two lineages, namely actinopterygians (bichirs, sturgeons, gars, bowfins and teleosts) and sarcopterygians (coelacanth, lungfishes and tetrapods). It remains unclear how the two osteichthyan lineages acquired their respective characters and how their common osteichthyan ancestor arose from non-osteichthyan gnathostome groups<sup>1,2</sup>. Here we present the first tentative reconstruction of a 400-million-year-old fossil fish from China (Fig. 1); this fossil fish combines features of sarcopterygians and actinopterygians and yet possesses large, paired fin spines previously found only in two extinct gnathostome groups (placoderms and acanthodians). This early bony fish provides a morphological link between osteichthyans and non-osteichthyan groups. It changes the polarity of many characters used at present in reconstructing osteichthyan inter-relationships and offers new insights into the origin and evolution of osteichthyans.

The fossil fish *Psarolepis romeri*<sup>3</sup> was described on the basis of skull and lower jaw materials from the Lower Devonian strata (about 400 million years (Myr) BP) of Qujing, Yunnan, China. Materials assignable to the same genus from the Upper Silurian (about 410 Myr BP) of China<sup>4</sup> and Vietnam<sup>5</sup> made *Psarolepis* one of the earliest osteichthyans known so far. The skulls and lower jaws exhibit the overall morphology of sarcopterygians but also show characters found in primitive actinopterygians, such as a tooth-bearing median rostral and a lower jaw with five coronoids (rather than three as in most sarcopterygians)<sup>3,6</sup>. *Psarolepis* was first placed within sarcopterygians, as a basal member of Dipnormorpha<sup>3</sup> or among the basal members of Crossopterygii<sup>4</sup>. The new features revealed by the shoulder girdle and cheek materials reported here (Figs 1d, e, 2, 3) indicate that *Psarolepis* may occupy a more basal position in osteichthyan phylogeny.

Most *Psarolepis* specimens derive from four beds at the same locality in Qujing, the first bed being in the Yulongsi Formation (Pridoli), the second and third beds in the Xishancun Formation (early Lochkovian), and the fourth bed in the Xitun Formation (late

Lochkovian). The specimens described here are from the second and third beds. The shoulder girdles and cheek plates from the third bed are often preserved as internal moulds (Fig. 2a) or as external moulds showing the internal casts of sensory canals and the pore-canal system (Figs 2b, c, 3a). Like elements previously assigned to *Psarolepis*<sup>3–5</sup>, these materials exhibit the unique ornamentation with large, closely spaced pores on the cosmine surface. This unique ornamentation forms the basis of their assignment to *Psarolepis*, which is also supported by other histological and morphological features and by their association with elements that are directly comparable to the type specimen.

The shoulder girdle (Fig. 2) bears a huge pectoral spine that extends posteriorly from a conspicuous ridge between the ventral and vertical laminae of the cleithrum, resembling the condition in some placoderms and acanthodians. In addition, the symmetrical fin spine<sup>4</sup> indicates that *Psarolepis* may possess median spines in front of the unpaired fins (Fig. 1a, c), as in sharks and acanthodians. The median fin spine exhibits the same ornamentation as the associated parietal shield and lower jaw<sup>4</sup>; other taxa from the same bed (petalichthyids and galeaspids) cannot possess a similar ornamentation. Such paired and unpaired fin spines are unknown in early osteichthyans, whether sarcopterygians or actinopterygians<sup>1</sup>. The only possible exceptions are two questionable Silurian forms, *Lophosteus*, which has indeterminate spine-like fragments<sup>7</sup>, and *Andreolepis*, which has a lateral projection of the cleithrum<sup>8,9</sup>.

A critical issue is whether *Psarolepis* has the typical sarcopterygian monobasal articulation of the paired fins. Although the internal mould of the endoskeletal shoulder girdle (Fig. 2a) does not show

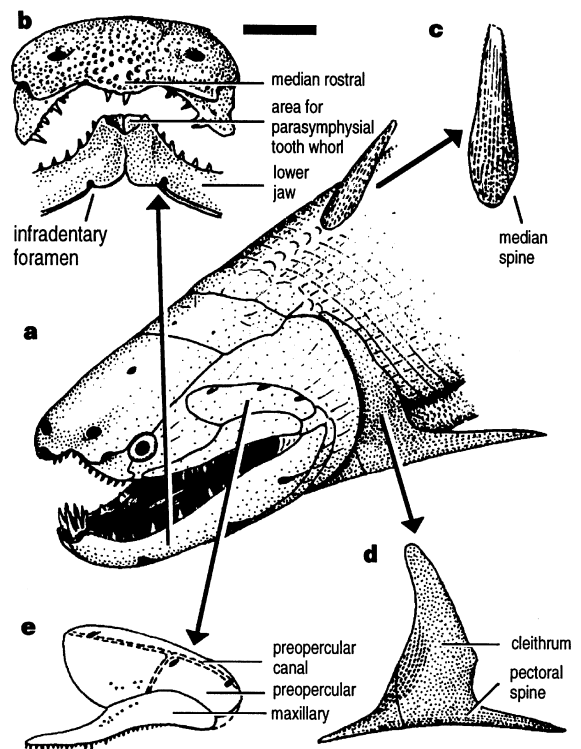


**Figure 1** Reconstruction of *Psarolepis*, a 400-million-year-old sarcopterygian-like fish with an unusual combination of osteichthyan and non-osteichthyan features. **a**, Head and anterior part of the fish with tentatively positioned median fin spine. **b**, Anterior view of the skull and lower jaws (from ref. 3). Scale bar, 5 mm. **c**, Median fin spine (from ref. 4). **d**, Shoulder girdle with pectoral spine, based on specimens shown in Fig. 2. **e**, Cheek plate with maxillary and preopercular, based on specimens shown in Fig. 3. Surface ornamentation of the cheek plate is omitted to show the pattern of sensory canals. Most *Psarolepis* specimens derive from four beds at the same locality in Qujing, Yunnan, China.

the articulation surface of the fin skeleton clearly, its overall shape is strikingly different from that of both sarcopterygians and actinopterygians. It is a massive, plate-shaped bone pierced internally by several openings for blood vessels and nerves, in many ways like the condition in placoderms. The anterior part of the cleithrum has a denticulate postbranchial lamina (Fig. 2b), as in placoderms and actinopterygians. In contrast, the dorsal part of the cleithrum is high and pointed, as in actinopterygians, onychodonts and primitive coelacanth; it is different from the broad dorsal apex found in lungfishes, porolepiforms and osteolepiforms.

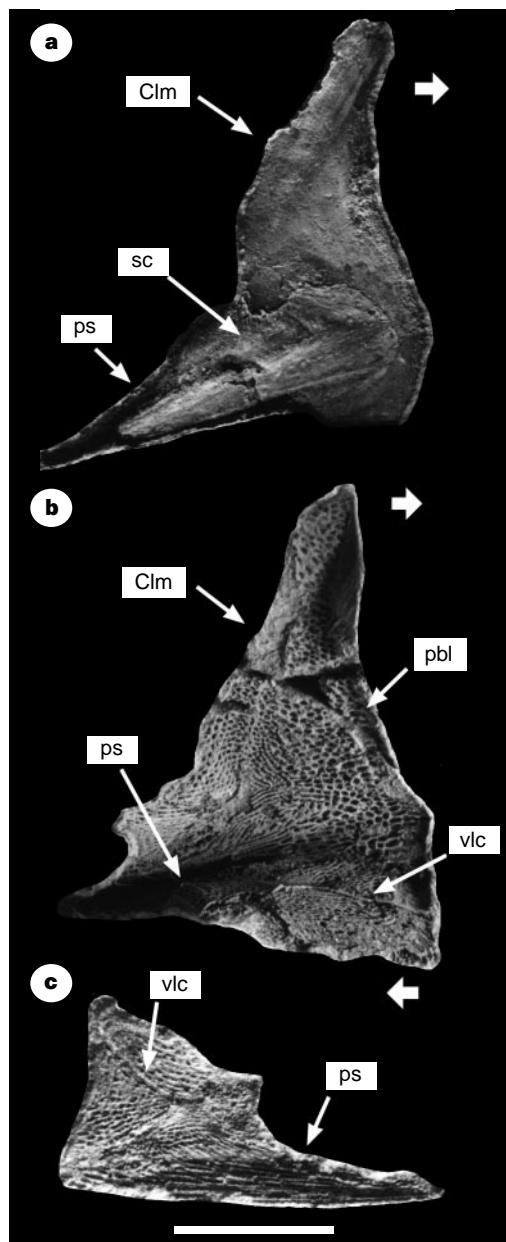


**Figure 2** Shoulder girdles of *Psarolepis*. **a**, Specimen IVPP V11256.1: internal mould of a right cleithrum with pectoral spine (ps) and scapulocoracoid (sc). **b**, Specimen IVPP V11256.3: external mould of a left cleithrum with pectoral spine. **c**, Specimen IVPP V11256.4: external mould of an incomplete left cleithrum with pectoral spine. All specimens derive from the third bed in the Xishancun Formation (early Lochkovian) and are associated with undescribed cranial and lower jaw elements directly comparable to the type specimen. Short, thick arrows point to the anterior end of the fish. Scale bar, 10 mm. See Fig. 1d for a simplified reconstruction. Clm, cleithrum; pbl, postbranchial lamina; vlc, internal cast of canal on ventral lamina of cleithrum.

The external mould of the cheek plate from the third bed (Fig. 3a) matches the shape of a large, tilted preopercular in the cheek plate from the second bed (Fig. 3b); this latter cheek plate also shows a posteriorly expanded maxillary. The preopercular lacks a jugal canal (present in placoderms, acanthodians and chondrichthyans) but has a complete preopercular canal running along the dorsal margin of the bone (as in chondrichthyans, acanthodians and actinopterygians). Near the midpoint of the preopercular canal, a short vertical canal extends ventrally to the ventral margin of the preopercular. The dorsal portion of the preopercular carries three large foramina, similar to those found in the dermal cheeks of *Youngolepis*<sup>10</sup> and *Kenichthys*<sup>11</sup> as well as in the lower jaws of *Psarolepis*<sup>3,4</sup>, *Youngolepis*<sup>10</sup>, *Powichthys*<sup>12</sup> and some porolepiforms<sup>13</sup>. In addition to actinopterygians, sarcopterygian onychodonts<sup>13</sup> also have a posteriorly expanded maxillary in broad contact with the preopercular. However, the presence of a complete preopercular canal, the lack of a jugal canal and the absence of a separate squamosal distinguish *Psarolepis* from all previously known sarcopterygians.

To examine the phylogenetic position of *Psarolepis* and its impact on osteichthyan relationships, we used the data set in ref. 14 to construct an expanded matrix with 37 taxa and 149 characters (see Methods). As the codings for four characters in ref. 14 were modified by data in ref. 4, we used the phylogenetic package PAUP<sup>15</sup> to analyse the expanded matrix twice, first with the modified codings from ref. 4, then with the original codings from

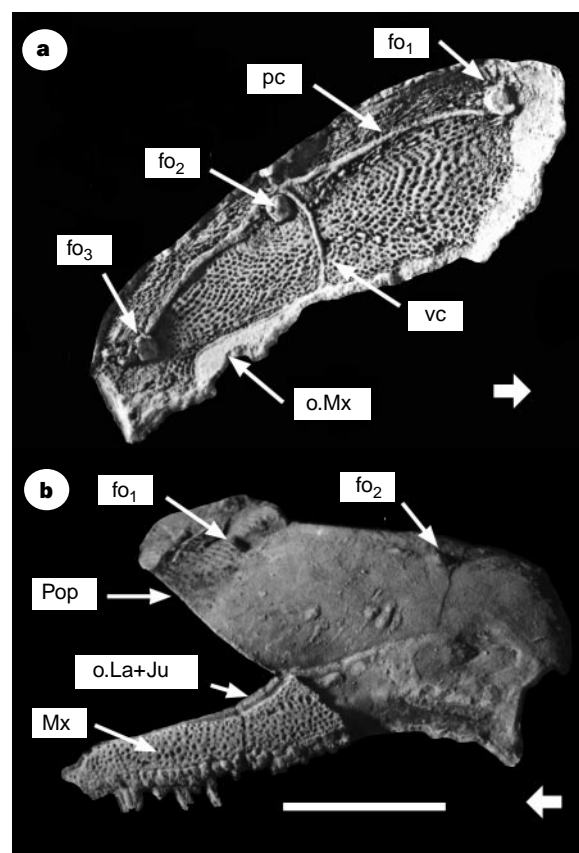


**Figure 3** Cheek bones of *Psarolepis*. **a**, Specimen IVPP V11256.2: external mould of a left preopercular with the internal cast of sensory canals (pc, vc) and the pore-canal system, from the third bed in the Xishancun Formation. **b**, Specimen IVPP V11255: lateral view of a left preopercular (Pop) and maxillary (Mx), from the second bed in the Xishancun Formation. Short, thick arrows point to the anterior end of the fish. Scale bar, 10 mm. See Fig. 1e for a simplified reconstruction. fo<sub>1</sub>–fo<sub>3</sub>, foramina of unknown function; o-La + Ju, area overlapped by lacrimal and jugal; o-Mx, area overlapped by maxillary; pc, internal cast of preopercular canal; vc, internal cast of vertical canal.

ref. 14. The strict consensus tree based on the modified codings in ref. 4 places *Psarolepis* as the sister group of all osteichthyans, whereas the strict consensus tree based on the original codings in ref. 14 places *Psarolepis* as the sister group of all previously known sarcopterygians (Fig. 4a, b). Figure 4c shows the two possible positions of *Psarolepis* and the incongruous distribution of *Psarolepis* features among the major gnathostome groups.

Although the clades common to the two competing schemes<sup>4,14</sup> of sarcopterygian interrelationships remain well supported, the conflicts between the two schemes remain unresolved and the exact position of *Psarolepis* remains uncertain. The uncertainty results partly from a lack of information available for *Psarolepis* and other

important stem taxa in the data set, and partly from the difficulty of selecting and polarizing characters when both osteichthyan and non-osteichthyan groups are used in the same analysis. However, whether *Psarolepis* turns out to be a stem-group osteichthyan or a stem-group sarcopterygian, its unique character combination will have a marked impact on present studies of osteichthyan evolution. For instance, porolepiform-like features found in *Psarolepis* (a lower jaw with three infradentary foramina, well developed internasal cavities and parasymphysial areas carrying tooth whorls<sup>3</sup>) can no longer be used to define porolepiforms<sup>16</sup> and/or dipnomorphs<sup>14</sup> (porolepiforms and lungfishes). The polyplacodont folded teeth and the quadrostian skull roof pattern of osteolepiforms<sup>3,17</sup> should

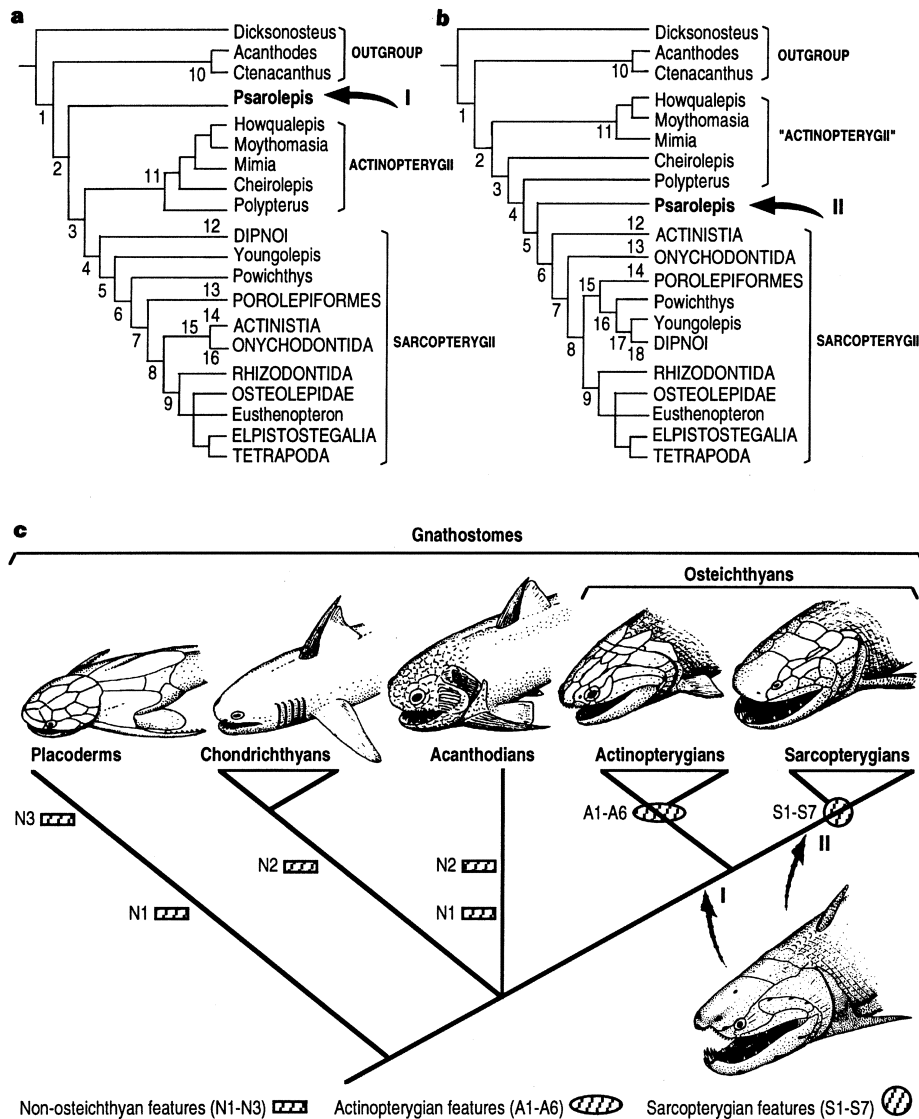


**Figure 4** Phylogenetic analysis and the incongruous distribution of *Psarolepis* characters. **a**, Strict consensus tree from the expanded character matrix based on data from ref. 4 (54 most parsimonious trees at 311 steps, consistency index = 0.543, retention index = 0.804). *Psarolepis* forms the sister group of all osteichthyans. **b**, Strict consensus tree from the expanded character matrix based on data from ref. 14 (54 most parsimonious trees at 314 steps, consistency index = 0.538, retention index = 0.798). *Psarolepis* forms the sister group of all previously known sarcopterygians. The internal topologies of Sarcopterygii in **a**, **b** match the respective topologies in refs 4, 14 (see Methods for details). The trees are simplified by omitting lower-level nodes within the higher terminal taxa shown in uppercase letters. **c**, Interpreted inter-relationships of major gnathostome groups showing the incongruous distribution of *Psarolepis* characters. Our analysis uses limited non-osteichthyan characters to study the position of *Psarolepis* rather

than the inter-relationships of non-osteichthyan gnathostomes. The sister-group relationship between *Acanthodes* and *Ctenacanthus* in **a**, **b** is converted to a trichotomy between chondrichthyans, acanthodians and osteichthyans to reflect our interpretation. Features: N1, bony pectoral spines; N2, median fin spine; N3, endoskeletal shoulder girdle as massive plate pierced by openings for blood vessels and nerves; A1, toothed median rostrai; A2, five coronoids in lower jaw; A3, absence of squamosal bone; A4, posteriorly expanded maxillary; A5, tilted preopercular with complete preopercular canal; A6, cleithrum with pointed vertical lamina; S1, lower jaw with three infradentary foramina; S2, well-developed internasal cavities; S3, parasymphysial area carrying tooth whorls; S4, polyplacodont teeth; S5, quadrostian skull roof pattern, S6, intracranial joint; S7, cosmine. See text for details.

also be regarded as primitive because of their presence in *Psarolepis*. If *Psarolepis* turns out to be a basal osteichthyan, the presence of an intracranial joint and cosmine can no longer serve as defining characters (synapomorphs) for sarcopterygians<sup>16–18</sup>. □

## Methods

**Phylogenetic analysis.** We added *Psarolepis* and three non-osteichthyan taxa (*Acanthodes*, an acanthodian, *Ctenacanthus*, a chondrichthyan, and *Dicksonosteus*, a placoderm) to the 33 taxa in ref. 14. We also added 9 characters to the 140 characters in ref. 14 to reflect the variations found in *Psarolepis* and the three non-osteichthyan outgroups (character 141, large dermal plates; 142, paired pectoral spines; 143, median fin spines; 144, denticulate postbranchial lamina of the cleithrum; 145, wide suborbital ledge; 146, eye stalk or unfinished area for similar structure; 147, ventral and otico-occipital fissures; 148, basiptyergoid articulation; 149, endochondral bone; 0 absent; 1 present). We adopted the same algorithm options as those used in refs 4, 14 (all characters unordered and unweighted) and used the three non-osteichthyan outgroups to root the trees. See Supplementary Information for the expanded matrix and for characters supporting major nodes in Fig. 4a, b. See ref. 14 for the original 140 characters and character states; see ref. 4 for the changed codings for characters 10, 17, 78 and 108.

Sarcopterygii, Dipnoi, Porolepiformes, Actinistia, Onychodontida and Tetrapodomorpha (including Rhizodontida, 'Osteolepiformes', Elpistostegalia and Tetrapoda) remain well supported in both trees. However, *Psarolepis* has changed the distribution and significance of many characters used previously to define osteichthyan groups (see Supplementary Information). In Fig. 4a, Sarcopterygii is defined by ten synapomorphies instead of fourteen as in ref. 14. Osteichthyes has no synapomorphy and is supported only by homoplasies. Actinopterygii is defined by one synapomorphy (character 6) and three reversals (characters 52, 93 and 110). In Fig. 4b, Sarcopterygii is defined by four synapomorphies, and 'Actinopterygii' appears as a paraphyletic group. One synapomorphy (character 7) defines the clade *Minimia* + (*Howqualepis* + *Moythomasia*) and five synapomorphies (characters 46, 63, 69, 98 and 134) define the clade *Polypterus* + (*Psarolepis* + Sarcopterygii). The position of *Polypterus* calls for further study, and the impact of data sampling and character coding on osteichthyan phylogeny deserves more attention.

Received 29 September 1998; accepted 7 January 1999.

1. Janvier, P. *Early Vertebrates* (Oxford Univ. Press, Oxford, 1996).
2. Rosen, D. E., Forey, P. L., Gardiner, B. G. & Patterson, C. Lungfishes, tetrapods, paleontology and plesiomorphy. *Bull. Am. Mus. Nat. Hist.* **167**, 159–276 (1981).
3. Yu, X. A new porolepiform-like fish, *Psarolepis romeri*, gen. et. sp. nov. (Sarcopterygii, Osteichthyes) from the Lower Devonian of Yunnan, China. *J. Vert. Paleontol.* **18**, 261–274 (1998).
4. Zhu, M. & Schultz, H.-P. The oldest sarcopterygian fish. *Lethaia* **30**, 293–304 (1997).
5. Tong-Duzay, T., Ta-Hoa, P., Boucot, A. J., Goujet, D. & Janvier, P. Vertébrés siluriens du Viet-nam central. *C.R. Acad. Sci.* **32**, 1023–1030 (1997).
6. Gardiner, B. G. The relationships of the palaeoniscid fishes, a review based on new specimens of *Mimia* and *Moythomasia* from the Upper Devonian of Western Australia. *Bull. Brit. Mus. Nat. Hist.* **37**, 173–428 (1984).
7. Otto, M. Zur systematischen Stellung der Lophosteiden (Obersilur, Pisces inc. sedis). *Paläont. Z.* **65**, 345–350 (1993).
8. Schultze, H.-P. Ausgangform und Entwicklung der rhombischen Schuppen der Osteichthyes (Pisces). *Paläont. Z.* **51**, 152–168 (1977).
9. Janvier, P. On the oldest known teleostome fish *Andreolepis hedei* Gross (Ludlow of Gotland), and the systematic position of the lophosteids. *Eesti NSV Teaduste Akadeemia Toimetised Geol.* **27**, 86–95 (1978).
10. Chang, M. M. in *Early Vertebrates and Related Problems of Evolutionary Biology* (eds Chang, M. M., Liu, Y. H. & Zhang, G. R.) 355–378 (Science Press, Beijing, 1991).
11. Chang, M. M. & Zhu, M. A new Middle Devonian osteolepidid from Qujing, Yunnan. *Mem. Ass. Australas. Palaeontol.* **15**, 183–198 (1993).
12. Jessen, H. L. Lower Devonian Porolepiformes from the Canadian Arctic with special reference to *Powichthys tharsteinsoni* Jessen. *Palaeontogr. Abt. A* **167**, 180–214 (1980).
13. Ahlberg, P. E. A re-examination of sarcopterygian interrelationships, with special reference to the Porolepiformes. *Zool. J. Linn. Soc.* **103**, 241–287 (1991).
14. Cloutier, R. & Ahlberg, P. E. in *Interrelationships of Fishes* (eds Stiassny, M. L., Parenti, L. R. & Johnson, G. D.) 445–480 (Academic, New York, 1996).
15. Swofford, D. L. PAUP: phylogenetic analysis using parsimony, version 3.1.1 (1993).
16. Jarvik, E. Basic structure and evolution of vertebrates. Vol. 2 (Academic, London, 1981).
17. Andrews, S. M. in *Interrelationships of Fishes* (eds Miles, R. S. & Patterson, C.) 137–177 (Academic, London, 1973).
18. Bjerring, H. The 'intercranial joint' vs the 'ventral otic fissure'. *Act. Zool. Stockh.* **59**, 203–214 (1978).

**Supplementary information** is available on Nature's World Wide Web site (<http://www.nature.com>) or as paper copy from the London editorial office of Nature.

**Acknowledgements.** We thank H.-P. Schultze, M. M. Chang and P. E. Ahlberg for useful discussions; W. Harre for the photographs and P. E. Ahlberg, M. I. Coates and M. M. Smith for comments and suggestions. M.Z. acknowledges support from the Alexander von Humboldt Foundation and the Chinese academy of Sciences. X.Y. thanks IVPF for access to specimens and Kean University for support for research and faculty development.

Correspondence and requests for materials should be addressed to M.Z. (e-mail: zhumin@ht.rol.cn.net).

## Influence of motion signals on the perceived position of spatial pattern

Shin'ya Nishida\* & Alan Johnston†

\* Human and Information Science Research Laboratory, NTT Communication Science Laboratories, 3-1, Morinosato-Wakamiya, Atsugi-shi, Kanagawa 243-0198, Japan

† Department of Psychology and Institute of Cognitive Neuroscience, University College London, Gower Street, London WC1E 6BT, UK

After adaptation of the visual system to motion of a pattern in a particular direction, a static pattern appears to move in the opposite direction—the motion aftereffect (MAE)<sup>1,2</sup>. It is thought that the MAE is not accompanied by a shift in perceived spatial position of the pattern being viewed<sup>3,4</sup>, providing psychophysical evidence for a dissociation of the neural processing of motion and position that complements anatomical and physiological evidence of functional specialization in primate and human visual cortex<sup>5–7</sup>. However, here we measure the perceived orientation of a static windmill pattern after adaptation to rotary motion and find a gradual shift in orientation in the direction of the illusory rotation, though at a rate much lower than the apparent rotation speed. The orientation shift, which started to decline within a few seconds, could persist longer than the MAE, and disappeared when the MAE was nulled by physical motion of the windmill pattern. Our results indicate that the representation of the position of spatial pattern is dynamically updated by neurons involved in the analysis of motion.

In the first experiment (see Methods), we investigated whether the MAE is accompanied by corresponding changes in apparent spatial position, and, if so, in what way the position shift changes over time. The results (Fig. 1) showed that after adaptation to a rotating windmill, a test windmill appeared to have rotated in the direction of the MAE. Using vernier tasks, T. Takeuchi (personal communication) and Snowden<sup>8</sup> have found shifts in position after motion adaptation. However, we also found that the shift in perceived orientation, which presumably resulted from local changes in apparent position, gradually increased over the first few seconds. An incremental change began at the test onset rather than at the adaptation offset, a finding reminiscent of the storage effect of the MAE<sup>9</sup>. Over the first two seconds, the orientation shift increased almost linearly; thus, for this interval, we can directly compare the rate of orientation change with the MAE speed. The gain, that is, the slope of the functions in Fig. 1 (0.40 and 0.65 degrees s<sup>-1</sup> for subjects SN and AJ, respectively) divided by the MAE speed measured separately (5.05 and 8.00 degrees s<sup>-1</sup>, respectively), was ~8%. These results show that the shift in orientation is not simply an alternative measure of the MAE and are consistent with the classical view that the perception of motion and that of position change are dissociated<sup>3</sup>. We rejected the idea that the magnitude of the orientation shift might be proportional to MAE strength, because we found that MAE speed did not increase as a function of time over the same interval (data not shown).

The shift in orientation started to decline a few seconds after the test onset. We measured the shift for a stationary test at repeated intervals for up to 2 min, and compared the decay function with that of the MAE (Fig. 2a) (experiment 2; see Methods). For two subjects the orientation shift decayed more slowly and persisted for longer than the MAE. Significant amounts of orientation shift remained even after the MAE finished. However, for another naïve subject, the decay functions of the orientation shift and the MAE were quite similar.